Journal of Quantitative Spectroscopy & Radiative Transfer 113 (2012) 221–225

Contents lists available at SciVerse ScienceDirect

Journal of Quantitative Spectroscopy & Radiative Transfer

journal homepage: www.elsevier.com/locate/jqsrt

Mid- and long-wave infrared absorption cross sections for acetonitrile

Jeremy J. Harrison *, Peter F. Bernath [1]

Department of Chemistry, University of York, Heslington, York YO10 5DD, United Kingdom

ARTICLE INFO

Article history:
Received 2 September 2011
Received in revised form
2 November 2011
Accepted 3 November 2011
Available online 9 November 2011

Keywords:
Acetonitrile
Methyl cyanide
High-resolution Fourier transform spectroscopy
Infrared absorption cross sections
Remote-sensing
Atmospheric chemistry

ABSTRACT

Infrared absorption cross sections for acetonitrile (methyl cyanide; CH_3CN) have been determined in the 880–1700 cm^{-1} spectral region from spectra recorded using a high-resolution FTIR spectrometer (Bruker IFS 125 HR) and a multipass cell with a maximum optical pathlength of 19.3 m. Spectra of acetonitrile/dry synthetic air mixtures were recorded at 0.015 cm^{-1} resolution (calculated as the Bruker instrument resolution of 0.9/MOPD) at a number of temperatures between 203 and 297 K and pressures appropriate for atmospheric conditions. Intensities were calibrated using three composite acetonitrile spectra recorded at the Pacific Northwest National Laboratory. These absorption cross sections will provide an accurate basis for upper tropospheric/lower stratospheric retrievals of acetonitrile in the mid-infrared spectral region from ACE satellite data.

© 2011 Elsevier Ltd. All rights reserved.

1. Introduction

Acetonitrile (CH_3CN) is a minor constituent of the Earth's atmosphere, with the majority of emissions arising from biomass burning [1–3]. A major sink for acetonitrile is wet removal in the troposphere and deposition in the ocean [4], with chemical loss primarily through the reaction with OH, which is rather slow. The lifetime of acetonitrile is of the order of 6 months [4,5], making this molecule a useful tracer for biomass burning and other atmospheric transport processes. In situ observations of tropospheric acetonitrile [4] have indicated typical background levels of 50–200 ppt (parts per trillion). In regions of forest fire activity, tropospheric mixing ratios are significantly enhanced [3]. The reader is referred to our previous paper on acetonitrile absorption cross sections in the 3 μm region [6] for a more detailed summary of the importance of acetonitrile in the atmosphere.

The first satellite measurements of acetonitrile in the Earth's atmosphere were taken by the Microwave Limb Sounder (MLS) instrument on the Upper Atmosphere Research Satellite (UARS) [7,8]. Acetonitrile has not yet been detected by satellite infrared (IR) remote sensing, largely due to a lack of appropriate IR spectroscopic data. Retrievals of concentration profiles from IR satellite data require accurate laboratory spectroscopic measurements in the form of either line parameters or absorption cross sections, which cover the range of atmospheric temperatures and pressures appropriate for the recorded satellite spectra. It is important that the laboratory spectra are recorded at a sufficient resolution, determined by the Doppler or pressure broadening, to resolve all the molecular features; this prevents errors in the retrieval when the forward model is convolved with the instrumental lineshape (ILS) function of the satellite Fourier transform spectrometer (FTS) instrument.

Rinsland et al. [9] have recorded a set of quantitative spectra at the Pacific Northwest National Laboratory (PNNL). These 29 spectra were measured at three different

* Corresponding author. Tel.: +44 1904 324589; fax: +44 1904 322516.
E-mail address: jeremy.harrison@york.ac.uk (J.J. Harrison).
[1] Present address: Department of Chemistry and Biochemistry, Old Dominion University, Norfolk, VA 23529, USA.

0022-4073/$ - see front matter © 2011 Elsevier Ltd. All rights reserved.
doi:10.1016/j.jqsrt.2011.11.003

temperatures (276 K, 298 K, and 323 K) and a number of different acetonitrile volume mixing ratios (VMRs) with 1 atm of N_2 as pressure broadening gas. Each spectrum covers the region 600–6500 cm^{-1} with a spectral resolution of 0.112 cm^{-1}. Despite not extending over the range of temperatures and pressures found in the upper troposphere/lower stratosphere (UTLS) and having been recorded at a moderate resolution (and due to the lack of any alternatives), these spectra were used to derive a pseudo-linelist between 870 and 1650 cm^{-1}, which was used to retrieve atmospheric profiles of acetonitrile from solar occultation spectra recorded by the MkIV balloon-borne interferometer (between 1993 and 2004) [10]. This was the first detection of acetonitrile in the Earth's atmosphere using IR remote sensing.

In addition to three composite spectra derived from the 29 PNNL spectra, the HITRAN database [11] also contains a set of line parameters for the ν_4 band (ν_0=920 cm^{-1}), derived from high-resolution room-temperature spectra [12]. These were primarily aimed at detecting acetonitrile in the atmosphere of Titan using Cassini's Composite Infrared Spectrometer (CIRS). Other stronger acetonitrile bands, such as the ν_6 band (ν_0=1450 cm^{-1}), are more suitable for remote sensing of the Earth's atmosphere.

The sparsity of quantitative low-temperature spectroscopic acetonitrile data for remote sensing purposes can be explained by the experimental difficulties involved in taking the measurements. Acetonitrile has a low vapour pressure (~1 Torr at 225 K and ~0.1 Torr at 200 K) [13], meaning that long optical pathlengths are required to achieve sufficient signal-to-noise ratios when performing spectroscopic measurements at low temperatures. In this work we utilise a multipass cell, achieving pathlengths as long as 19.3 m.

This work follows on from Ref. [6], providing quantitative spectroscopic data in the mid- and long-wave infrared (MWIR; LWIR) regions. In a similar manner to these and previous measurements [14–17], high-resolution (0.015 cm^{-1}) spectra of acetonitrile/dry synthetic air have been recorded over a range of pressures and temperatures (50–760 Torr and 203–297 K), and used to derive absorption cross sections between 880 and 1700 cm^{-1}. These can be used to retrieve acetonitrile profiles from satellite instruments recording IR spectra through the atmosphere, in particular atmospheric limb spectra recorded by the ACE-FTS instrument onboard the SCISAT-1 satellite. Currently the ACE-FTS, which covers the spectral region from 750 to 4400 cm^{-1}, can detect more organic molecules in the UTLS than any other satellite instrument [18].

2. Experimental

Air-broadened acetonitrile absorption spectra were recorded at the Molecular Spectroscopy Facility (MSF), Rutherford Appleton Laboratory (located in Oxfordshire, UK), using a Bruker Optics IFS 125HR high-resolution Fourier transform spectrometer (FTS) with an internal mid-infrared radiation source (globar), a potassium bromide beamsplitter, a mercury cadmium telluride (MCT) detector, and an optical filter restricting the throughput to the spectral region below 1800 cm^{-1} and above the detector cut-off at 690 cm^{-1}. The FTS was set to a resolution of 0.015 cm^{-1} (calculated as the Bruker instrument resolution of 0.9/MOPD), with the aperture diameter (3.15 mm) chosen so that the intensity of infrared radiation falling on the detectors was maximised without saturation or loss of spectral resolution. Norton–Beer weak apodisation and Mertz phase corrections were applied to all interferograms. Due to the non-linear response of MCT detectors to the detected radiation, which results in baseline perturbations, all interferograms were re-transformed using the non-linearity correction in Bruker's OPUS software. The FTS instrumental parameters and settings are summarised in Table 1.

The MSF short-path absorption cell (SPAC), which has previously been used for measurements of acetone [16,17] and acetonitrile (in the 3 μm region) [6], was used for all measurements. The SPAC is a coolable, multipass White cell, with two externally adjustable mirrors, capable of achieving an optical pathlength between 1.7 m and 19.3 m (in steps of 1.6 m). Transfer optics are used to transfer the radiation from the spectrometer into the cell, and from the cell onto the external MCT detector. These transfer optics are housed in chambers evacuated to pressures of less than 0.02 Pa in order to minimise the absorbance of impurity atmospheric gases in the optical path. For a similar reason, the FTS itself is evacuated to a pressure below 0.2 Pa.

Dissolved air was removed from a sample of acetonitrile (Fluka, ≥99.8% purity) in a small Pyrex glass tube using multiple freeze-pump-thaw cycles with liquid N_2. A small amount of cold acetonitrile vapour was then introduced into the SPAC via a gas-handling line. Sample mixtures were prepared by adding dry synthetic air ('Air Zero Plus', Air Products, 99.99990% overall purity; used without additional purification) to the acetonitrile vapour. Both cell and gas-line were evacuated by a turbomolecular vacuum pump between measurements.

In these experiments the SPAC was operated from room temperature down to 203 K. For each measurement, the actual cell temperature (which can be automatically controlled for extended periods of time) was monitored by six platinum resistance thermometers situated at positions

Table 1
FTS and SPAC configurations.

Source	Globar
Detector	Mercury cadmium telluride (MCT)
Beam splitter	Potassium bromide (KBr)
Resolution	0.015 cm^{-1}
Aperture size	3.15 mm
Optical filter	LP 5.75 μm (Northumbria Optical Coatings Ltd.)
Apodisation function	Norton–Beer Weak
Phase correction	Mertz
Cell windows	Barium fluoride (BaF_2)
Transfer optics chamber windows	Potassium bromide (KBr)
Mirror coatings	Gold
Pressure gauges	3 MKS-690A Baratrons (1, 10, and 1000 Torr) (±0.05% accuracy)
Thermometry	6 PRTs, Labfacility IEC 751 Class A

Table 2
Summary of the sample conditions for all scans.

Temperature (K)	Initial acetonitrile pressure (Torr)[a]	Total pressure (Torr)	Pathlength[b] (m)	No. of scans[c]
203.6 ± 1.2	0.0043	49.82 ± 0.10	19.31	400
203.3 ± 0.9	0.0043	75.13 ± 0.15	19.31	400
203.2 ± 0.8	0.0043	100.40 ± 0.15	19.31	700
215.0 ± 1.0	0.0400	51.18 ± 0.15	19.31	300
214.6 ± 0.7	0.0400	104.56 ± 0.15	19.31	330
214.5 ± 0.5	0.0400	259.9 ± 0.3	19.31	290
249.5 ± 0.5	0.4777	200.65 ± 0.15	1.71	300
249.5 ± 0.5	0.5343	399.6 ± 0.4	1.71	310
249.5 ± 0.4	0.5343	602.1 ± 0.5	1.71	300
274.9 ± 0.7	0.8065	369.9 ± 0.7	1.71	300
274.8 ± 0.3	0.8910	600.6 ± 0.4	1.71	300
297.1 ± 0.2	1.093	759.8 ± 0.3	1.71	290

[a] MKS-690A Baratron readings are accurate at ± 0.05%.
[b] The error in the optical pathlength is estimated to be ± 0.2% at room temperature.
[c] Note that each sample requires the measurement of a similar number of background scans taken with the same spectrometer settings. One scan takes about 33 s.

throughout the inner sample vessel of the SPAC. The pressure in the cell was measured by three MKS-690A Baratron capacitance manometers (full scale 1, 10, and 1000 Torr) connected to the gas line, close to the SPAC inlet.

Details of the pressures, temperatures, optical pathlengths, and the number of scans taken for each sample are provided in Table 2. Additionally, evacuated-cell background scans were recorded before and after the scan blocks for each sample, and scans of pure N_2O were recorded at each temperature to calibrate the frequency scale. The temperatures and pressures of the sample mixtures were logged by computer every few seconds. The variations in these quantities were used to estimate their experimental uncertainties (see Table 2). The acetonitrile partial pressures cannot be monitored in the same way, so Table 2 lists the initial pressures before the addition of synthetic air. Once each acetonitrile/dry synthetic air mixture reaches thermal equilibrium, the temperature (and hence the absorber amount) has changed slightly from when the initial acetonitrile pressure reading was taken. This discrepancy between the initial recorded pressure and the actual partial pressure in the cell is difficult to quantify, but the effect is largest at the lowest temperatures, where the vapour pressure of acetonitrile changes rapidly with temperature. This is one of the reasons why we normalise the measurements against an accurate intensity standard, in this case the PNNL acetonitrile spectra [9]. This is discussed further in Section 3.

3. Results and discussion

Sinusoidal modulations in the spectral domain, also known as channel fringes, were present in all the recorded single channel scans. These are caused by reflections from optical components such as cell or transfer-optics windows, having the effect of introducing weaker centreburst 'echoes' into the interferogram, which appear in the spectrum as sinusoidal modulations (once the interferogram is Fourier transformed). Channel fringes were observed in previous MWIR acetone measurements using the same apparatus [17]. Like these previous measurements, the frequency components of the oscillations varied slightly from scan to scan. Under such circumstances, transmission spectra cannot be calculated simply by dividing single-channel sample and background scans.

The channelling was removed using the same method as for the MWIR acetone scans [17]. Briefly, for background scans the appropriate 'ghost' peaks were simply removed from the interferogram before Fourier transforming into the spectral domain. However, simply removing 'ghost' peaks from a sample interferogram introduces artefacts into the spectrum. For sample scans, channelling components were removed one at a time by stretching and shifting the associated periodic oscillations of the corresponding component from a background spectrum until they matched as closely as possible. After simple division, channel fringes were removed from the sample scans to within the noise level. Transmission spectra were calculated in the usual manner, with a further small correction required to position the baseline correctly. These spectra have typical signal-to-noise ratios (RMS) ranging from 500 to 800.

Spectral frequencies were calibrated using pure N_2O spectra recorded during the experimental run. Line positions of isolated N_2O absorption lines between 1140 and 1320 cm^{-1}, with an accuracy of between 0.001 and 0.0001 cm^{-1}, were taken from the HITRAN 2008 database [11].

Despite care being taken to prevent impurities entering the cell by using high purity gases and pumping out the gas line before the preparation of sample mixtures, absorption lines of water in the region 1300–1700 cm^{-1} were observed in the sample scans. These lines were removed individually by spectral simulation using parameters from the HITRAN 2008 database. Any obvious leftover 'residuals' were adjusted by hand to achieve the best possible result. It should be noted that these water lines are the same strong/saturated lines observed in atmospheric spectra. For the purposes of determining acetonitrile abundances in the Earth's atmosphere, the absorption cross sections are most useful in the regions between these water lines.

In principle, one could obtain an estimate of the random errors by taking many measurements at each temperature and (broadening) pressure combination, as is the case for measurements in the PNNL IR database [19]. In this work, we measure one acetonitrile concentration for each combination due to time constraints, the need to maximise the signal-to-noise at the longest pathlengths, large uncertainties in the amount of absorber in the cell at the lowest temperatures, and the unknown temperature dependence of the pathlength (when the SPAC is cooled down, the optics and mirrors within the cell shift position as they contract; the error in the SPAC optical pathlength is estimated to be ± 0.2% at room temperature). For these reasons, we choose to calibrate the *y*-axes of the cross sections derived in this work using the three composite acetonitrile spectra derived from the work of Rinsland et al. [9]. Here, we make use of the assumption that band

intensities for isolated bands comprising primarily fundamentals are independent of temperature [14,20]. Although overtones, combination bands, and hot bands can have small temperature dependences, these are much weaker for fundamental bands and their contributions to the overall integrated band intensity are small. In fact, the three composite PNNL spectra measured at 276 K, 298 K, and 323 K show no evidence of temperature dependence.

Spectral absorption cross sections, $\sigma(\upsilon, P_{air}, T)$, with units cm^2 $molecule^{-1}$, were calculated by the equation:

$$\sigma(\upsilon,P_{air},T) = -\xi \frac{10^4 k_B T}{Pl} \ln \tau(\upsilon,P_{air},T) \quad (1)$$

where $\tau(\upsilon, P_{air}, T)$ is the transmittance at wavenumber υ (cm^{-1}), synthetic air pressure P_{air}, and temperature T (K), P is the pressure of the absorbing gas (Pa), l is the optical pathlength (m), k_B is the Boltzmann constant ($=1.3806504\times10^{-23}$ J K^{-1}), and ξ is the factor required to satisfy the normalisation requirement:

$$\int_{1190\,cm^{-1}}^{1690\,cm^{-1}} \sigma(\upsilon,P_{air},T) = 3.898 \times 10^{-18}\,cm\,molecule^{-1}\ (\pm 0.3\%) \quad (2)$$

The value on the right hand side of Eq. (2) is the average integrated band strength of the three acetonitrile PNNL spectra (recorded at 276, 298, and 323 K) in the range 1190–1690 cm^{-1}, converted from PNNL units (ppm^{-1} m^{-1} at 296 K) using the factor $k_B \times 296 \times \ln 10 \times 10^4/0.101325$. The uncertainty in parentheses represents the spread from the mean of the three PNNL integrated band intensities. In order to minimise errors, this integral is taken over the ν_6 band, which possesses the best signal-to-noise ratio.

Fig. 1 is a plot over the entire recorded spectral range for the absorption cross section at 215.0 K and 51.2 Torr. The derived cross sections cover a number of acetonitrile vibrational band systems. The strongest of these is the ν_6 band ($\nu_0=1450$ cm^{-1}), associated with the CH_3 degenerate deformation [21], followed by the ν_7 band ($\nu_0=1042$ cm^{-1}; CH_3 rocking), and the ν_4 band ($\nu_0=920$ cm^{-1}; CC stretch). Additionally, the ν_6 band overlaps with the much weaker ν_3 band ($\nu_0=1385$ cm^{-1}) and the $\nu_7+\nu_8$ combination band ($\nu_0=1409$ cm^{-1}). Fig. 2 shows a plot of the three cross sections at ~215 K and 51.2, 104.6, and 259.9 Torr in the vicinity of the strongest ν_6 band feature at 1463 cm^{-1}, revealing obvious pressure broadening. This feature was used in the retrieval of atmospheric profiles of acetonitrile from MkIV solar occultation spectra [10].

Uncertainties in the sample temperatures and total pressures range from 0.07% to 0.6% and 0.04% to 0.3%, respectively (Table 2). The photometric uncertainty is estimated to be 1–2%. The pathlength error at room temperature is estimated to be 0.2%, increasing slightly as the cell is cooled because the mirrors and optical components change position as they contract. Any systematic error in the pathlength is accounted for by normalising the integrated band intensities against the three PNNL acetonitrile spectra, which have a stated experimental accuracy of 3.5% (1σ). We

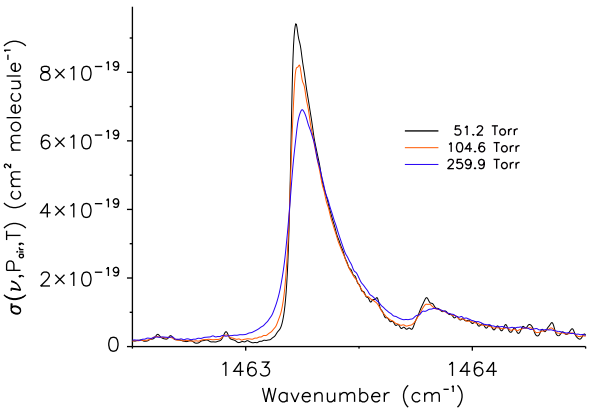

Fig. 2. Acetonitrile absorption cross sections at ~215 K and 51.2, 104.6, and 259.9 Torr in the vicinity of the strongest feature in the ν_6 band at 1463 cm^{-1}.

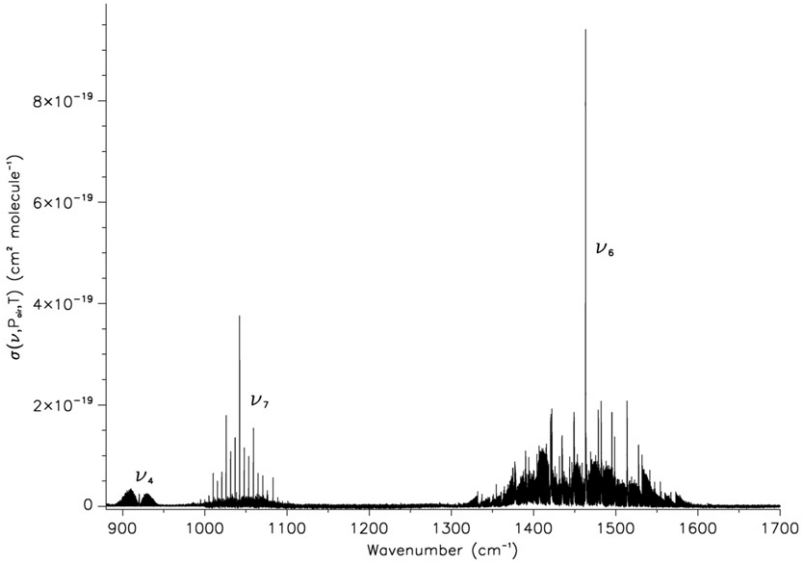

Fig. 1. Acetonitrile absorption cross section at 215.0 K and 51.2 Torr.

estimate an overall uncertainty in the new acetonitrile cross sections of 6% (1σ).

This set of spectral absorption cross sections (with a total zero filling factor of 4) for acetonitrile is available electronically upon request from the authors.

4. Conclusions

High-resolution infrared absorption cross sections for acetonitrile (between 880 and 1700 cm^{-1}) have been determined with an estimated uncertainty of 6%. Spectra were recorded for mixtures of acetonitrile with dry synthetic air at 0.015 cm^{-1} resolution using a range of temperatures and pressures appropriate for UTLS conditions and a multipass cell with a maximum optical pathlength of 19.3 m. Intensities were calibrated against three acetonitrile spectra taken from the PNNL IR database. The cross sections will enable retrievals of acetonitrile from atmospheric spectra recorded by IR remote sensing instruments onboard satellites, such as the ACE-FTS.

Acknowledgements

The authors wish to thank the Natural Environment Research Council (NERC) for supporting J.J. Harrison through Grant NE/F002041/1, and for access to the Molecular Spectroscopy Facility (MSF) at the Rutherford Appleton Laboratory (RAL). R.G. Williams and R. McPheat are thanked for providing technical support at the RAL.

References

[1] Holzinger R, Warneke C, Hansel A, Jordan A, Lindinger W, Scharffe DH, et al. Biomass burning as a source of formaldehyde, acetaldehyde, methanol, acetone, acetonitrile, and hydrogen cyanide. Geophysical Research Letters 1999;26:1161–4.

[2] Lobert JM, Scharffe DH, Hao WM, Crutzen PJ. Importance of biomass burning in the atmospheric budgets of nitrogen-containing gases. Nature 1990;346:552–4.

[3] de Gouw JA, Warneke C, Parrish DD, Holloway JS, Trainer M, Fehsenfeld FC. Emission sources and ocean uptake of aceotnitrile (CH_3CN) in the atmosphere. Journal of Geophysical Research 2003;108:4329, doi:10.1029/2002JD002897.

[4] Singh HB, Salas L, Herlth D, Kolyer R, Czech E, Viezee W, et al. In situ measurements of HCN and CH_3CN over the Pacific Ocean: sources, sinks, and budgets. Journal of Geophysical Research 2003;108:8795, doi:10.1029/2002JD003006.

[5] Li QB, Jacob DJ, Yantosca RM, Heald CL, Singh HB, Koike M, et al. A global three-dimensional model analysis of the atmospheric budgets of HCN and CH_3CN: constraints from aircraft and ground measurements. Journal of Geophysical Research 2003;108:8827, doi:10.1029/2002JD003075.

[6] Allen NDC, Harrison JJ, Bernath PF. Acetonitrile (CH_3CN) infrared absorption cross sections in the 3 μm region. Journal of Quantitative Spectroscopy and Radiative Transfer 2011;112:1961–6.

[7] Livesey NJ, Waters JW, Khosravi R, Brasseur GP, Tyndall GS, Read WG. Stratospheric CH_3CN from the UARS Microwave Limb Sounder. Geophysical Research Letters 2001;28:779.

[8] Livesey NJ, Fromm MD, Waters JW, Manney GL, Santee ML, Read WG. Enhancements in lower stratospheric CH_3CN observed by the Upper Atmosphere Research Satellite microwave limb sounder following boreal forest fires. Journal of Geophysical Research 2004;109:D06308, doi:10.1029/2003JD004055.

[9] Rinsland CP, Sharpe SW, Sams RL. Temperature-dependent infrared absorption cross sections of methyl cyanide (acetonitrile). Journal of Quantitative Spectroscopy and Radiative Transfer 2005;96:271.

[10] Kleinbohl A, Toon GC, Sen B, Blavier J-FL, Weisenstein DK, Wennberg PO. Infrared measurements of atmospheric CH_3CN. Geophysical Research Letters 2005;32:L23807, doi:10.1029/2005GL024283.

[11] Rothman LS, Gordon IE, Barbe A, Benner DC, Bernath PF, Birk M, et al. The HITRAN 2008 molecular spectroscopic database. Journal of Quantitative Spectroscopy and Radiative Transfer 2009;110:533–72.

[12] Rinsland CP, Malathy DV, Benner CD, Blake TA, Sams RL, Brown LR, et al. Multispectrum analysis of the nu4 band of CH_3CN: positions, intensities, self- and N_2-broadening, and pressure-induced shifts. Journal of Quantitative Spectroscopy and Radiative Transfer 2008;109:974–94.

[13] Yaws Carl L. Chemical properties handbook. McGraw-Hill; 1999.

[14] Harrison JJ, Allen NDC, Bernath PF. Infrared absorption cross sections for ethane (C_2H_6) in the 3 μm region. Journal of Quantitative Spectroscopy and Radiative Transfer 2010;111:357–63, doi:10.1016/j.jqsrt.2009.09.010.

[15] Harrison JJ, Bernath PF. Infrared absorption cross sections for propane (C_3H_8) in the 3 μm region. Journal of Quantitative Spectroscopy and Radiative Transfer 2010;111:1282–8, doi:10.1016/j.jqsrt.2009.11.027.

[16] Harrison JJ, Allen NDC, Bernath PF. Infrared absorption cross sections for acetone (propanone) in the 3 μm region. Journal of Quantitative Spectroscopy and Radiative Transfer 2011;112:53–8, doi:10.1016/j.jqsrt.2010.08.011.

[17] Harrison JJ, Humpage N, Allen NDC, Waterfall AM, Bernath PF, Remedios JJ. Mid-infrared absorption cross sections for acetone (propanone). Journal of Quantitative Spectroscopy and Radiative Transfer 2011;112:457–64, doi:10.1016/j.jqsrt.2010.09.002.

[18] Bernath PF, McElroy CT, Abrams MC, Boone CD, Butler M, Camy-Peyret C, et al. Atmospheric Chemistry Experiment (ACE): mission overview. Geophysical Research Letters 2005;32:L15S01, doi:10.1029/2005GL022386.

[19] Sharpe SW, Johnson TJ, Sams RL, Chu PM, Rhoderick GC, Johnson PA. Gas-phase databases for quantitative infrared spectroscopy. Applied Spectroscopy 2004;58:1452–61.

[20] Breeze JC, Ferriso CC, Ludwig CB, Malkmus W. Temperature dependence of the total integrated intensity of vibrational–rotational band systems. Journal of Chemical Physics 1965;42:402–6.

[21] Shimanouchi T. Molecular vibrational frequencies. In: Linstrom PJ, Mallard WG, editors. NIST chemistry webbook, NIST standard reference database number 69. Gaithersburg, MD 20899: National Institute of Standards and Technology; 2005, 〈http://webbook.nist.gov/〉.